Smart Structures and Systems, *Vol. 17, No. 6 (2016) 859-880*
DOI: http://dx.doi.org/10.12989/sss.2016.17.6.859

Damage detection of a cable-stayed bridge based on the variation of stay cable forces eliminating environmental temperature effects

Chien-Chou Chen[*1], Wen-Hwa Wu[1], Chun-Yan Liu[2] and Gwolong Lai[1]

[1]*Department of Construction Engineering, National Yunlin University of Science and Technology, 123 University Road, Touliu, Yunlin 640, Taiwan*
[2]*Graduate School of Engineering Science and Technology, National Yunlin University of Science and Technology, 123 University Road, Touliu, Yunlin 640, Taiwan*

(Received December 7, 2015, Revised March 23, 2016, Accepted March 28, 2016)

Abstract. This study aims to establish an effective methodology for the detection of instant damages occurred in cable-stayed bridges with the measurements of cable vibration and structural temperatures. A transfer coefficient for the daily temperature variation and another for the long-term temperature variation are firstly determined to eliminate the environmental temperature effects from the cable force variation. Several thresholds corresponding to different levels of exceedance probability are then obtained to decide four upper criteria and four lower criteria for damage detection. With these criteria, the monitoring data for three stay cables of Ai-Lan Bridge are analyzed and compared to verify the proposed damage detection methodology. The simulated results to consider various damage scenarios unambiguously indicate that the damages with cable force changes larger than ±1% can be confidently detected. As for the required time to detect damage, it is found that the cases with ±2% of cable force change can be discovered in no more than 6 hours and those with ±1.5% of cable force change can be identified in at most 9 hours. This methodology is also investigated for more lightly monitored cases where only the air temperature measurement is available. Under such circumstances, the damages with cable force changes larger than ±1.5% can be detected within 12 hours. Even though not exhaustively reflecting the environmental temperature effects on the cable force variation, both the effective temperature and the air temperature can be considered as valid indices to eliminate these effects at high and low monitoring costs.

Keywords: cable-stayed bridge; cable force; effective temperature; daily variation; long-term variation; transfer coefficient; damage detection; air temperature

1. Introduction

Several vibration-based damage detection methods recently developed have shown that structural health monitoring (SHM) is one of the feasible solutions to effectively assess the structural condition of bridges (Whelan and Janoyan 2010, Cunha *et al*. 2013, Dohler *et al*. 2014, Trker and Bayraktar 2014). The accuracy of SHM techniques in practical applications for bridge damage diagnosis, however, remains to be further improved and more extensively investigated.

∗Corresponding author, Associate Professor, E-mail: ccchen@yuntech.edu.tw

http://www.techno-press.org/?journal=sss&subpage=8 ISSN: 1738-1584 (Print), 1738-1991 (Online)

For cable-stayed bridges where the stay cable system plays the most crucial role to transmit loads, it is no doubt that the change of structural condition would induce the force redistribution of the cable system and the monitoring of cable force can be regarded as a royal road to diagnose possible damages. Nevertheless, environmental effects can also cause evident variation of cable force to complicate the whole problem. A number of studies (Ni *et al*. 2005, Ni *et al*. 2007, Min *et al*. 2009, Degrauwe *et al*. 2009, Chen *et al*. 2010) for cable-stayed bridges consistently indicated that temperature is typically the most dominant environmental factor to alternate the structural status. As a result, the success of SHM approaches for the damage detection of cable-stayed bridges strongly depends on accurate quantification of such an environmental temperature influence.

Even though enormous efforts based on laboratory and field tests have been attempted to identify or simulate the environmental temperature effects (Xu and Wu 2007, Ni *et al*. 2008, Ni *et al*. 2009, Li 2009, Zhou *et al*. 2010, Min *et al*. 2011, Cao *et al*. 2011, Sun *et al*. 2012, Yao and Li 2012, Zhou *et al*. 2013, Ding *et al*. 2013), only a few of these works (Degrauwe *et al*. 2009, Li 2009, Cao *et al*. 2011, Zhou *et al*. 2013) were focused on inspecting the cable force variation caused by the change of temperature. In order to more comprehensively explore this problem, the authors lately conducted a long-term monitoring on the cable forces and temperatures in various structural components of Ai-Lan Bridge, a cable-stayed bridge located in central Taiwan (Chen *et al*. 2012). It was discovered that an effective temperature defined to combine all the contributions from stay cable, bridge girder, and pylon based on a simplified model is strongly correlated with the cable force. Using these data collected from Ai-Lan Bridge, a recent work by the authors further applied the ensemble empirical mode decomposition (EEMD) to process the variation histories of the cable force and the effective temperature (Chen *et al*. 2014, Chen *et al*. 2015). It was clearly observed that the cable force and effective temperature can both be categorized as the daily variation, long-term variation, and high-frequency noise in the order of decreasing weight. Moreover, the correlation analysis conducted for the decomposed variations of both quantities indisputably disclosed that the daily and long-term variations with different time shifts have to be distinguished for accurately evaluating the temperature effects on the variation of cable force.

After successful identification and simulation of environmental temperature effects, the next goal naturally moves toward discriminating or even eliminating them from the variation of dynamic structural features for accurate damage detection. This progress has been made by a couple of studies in the literature for the applications in cable-stayed bridges. Ding *et al*. (2010) proposed a multi-stage scheme for structural damage detection of Runyang Bridge in China by extracting the wavelet packet energy spectrum (WPES) from the bridge measurements. Correlation models were formulated to describe the seasonal relationship between WPES and temperature for clear classification of the changes in WPES either due to environmental temperature or to structural damage. More recently, Zhou *et al*. (2012) developed a parametric approach for eliminating the temperature effect in vibration-based structural damage detection and applied it to Ting Kau Bridge in Hong Kong using long-term monitoring data. A correlation model between damage-sensitive modal features and temperature was firstly formulated with the neural network technique. With this correlation model, the modal features measured under different temperature conditions were then normalized to an identical reference status of temperature to eliminate the temperature effect.

Based on the previous research by the authors (Chen *et al*. 2014, Chen *et al*. 2015), the current study aims to establish an SHM methodology for the detection of instant damages occurred in cable-stayed bridges with the measurements of cable vibration and structural temperatures. A

transfer coefficient for the daily temperature variation and another for the long-term temperature variation are firstly determined by using the technique of least square errors. The environmental temperature effects can then be excluded from the variation history of cable force with these two transfer coefficients. Subsequently, statistical analysis is performed to define a few thresholds corresponding to different levels of exceedance probability and then decide the appropriate criteria for damage detection. The monitoring data for three stay cables of Ai-Lan Bridge with different lengths in each of the four seasons are analyzed and compared to verify the effectiveness of the proposed methodology. Finally, the developed methodology is also extended to the applications where merely the air temperature measurement is available with the SHM system.

2. Review of previous work

The recent work (Chen *et al*. 2014, Chen *et al*. 2015) by the authors to systematically assess the environmental temperature effects on the variation of stay cable force is firstly reviewed in this section to provide an informative background for the subsequent analysis.

2.1 Measurements of cable force and temperatures for Ai-Lan Bridge

Ai-Lan Bridge is a 3-span symmetric concrete cable-stayed bridge with a main span of 140 m. Nine pairs of stay cables on each side of every pylon are arranged in a harp shape along the centerline of girder, as illustrated in Fig. 1. A monitoring system was established during the construction stage to measure a number of important quantities including the temperature variations of surrounding air, girder, and pylon. In addition to the existing monitoring system, a simple device composed of a fiber Bragg grating (FBG) sensor attached on a fishing line (Chen *et al*. 2008) was developed by this research group to conduct the ambient vibration measurements of the cable. These FBG sensors were installed on Cables E01 to E18, all the 9 pairs of cables on G2 side of Pylon P1. From those signals, the natural frequencies of each cable can be identified and then employed to determine the corresponding cable forces with the ambient vibration method. Since no temperature sensors were deployed to take the cable temperature in the original monitoring system, a cable specimen of 1 m long was also made by this research group for imitating the real cable with assembling the same number of tendons inside an HDPE tube (Chen *et al*. 2012). FBG temperature sensors were attached on the surface of four inside strands to intimately take the temperature of the cable specimen placed on the bridge deck.

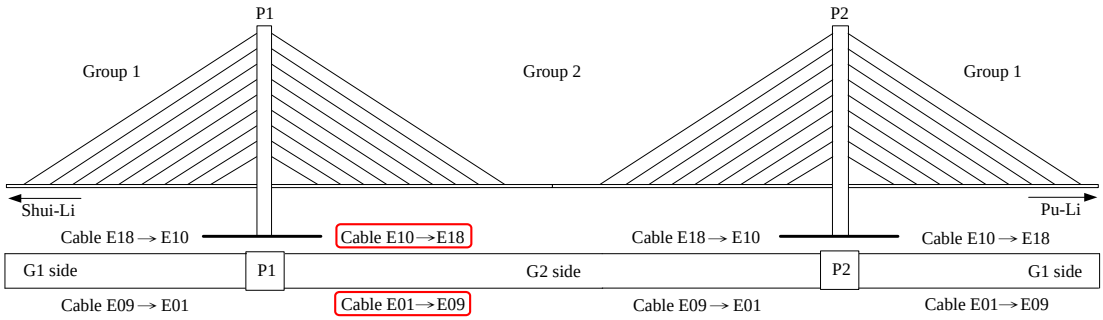

Fig. 1 Cable system of Ai-Lan Bridge

With the abovementioned measurement system, the vibration signal from the FBG sensor installed on each cable was automatically collected for 300 sec every 15 minutes. The obtained displacement time history of cable vibration is firstly transformed into the frequency domain by the discrete Fourier transform (DFT) technique. The cable frequencies can then be conveniently identified without ambiguity from the corresponding Fourier amplitude spectrum (FAS). Consequently, there are totally 96 sets of identified frequency values for each cable per day. In other words, the time increment $\Delta t = 15$ minutes. Because of several technical problems ever encountered with the installed FBG system, there were totally 246 days of effective signals intermittently collected from November of 2011 to October of 2012. Fortunately, at least 21 days of continuous data can still be extracted for each of the four seasons.

2.2 Effective temperature and stay cable force

Based on the string theory, it can be easily shown that

$$\frac{\Delta F}{F_1} = \frac{F_i - F_1}{F_1} = \frac{f_{ni}^2 - f_{n1}^2}{f_{n1}^2} = \frac{\Delta f_n^2}{f_{n1}^2} = \frac{\varepsilon_i - \varepsilon_1}{\varepsilon_1} = \frac{\Delta \varepsilon}{\varepsilon_1} \tag{1}$$

where F_1 and F_i stand for the stay cable force at an initial reference time t_1 and at any other time instant t_i, respectively. Corresponding to these two time instants, f_{n1} and f_{ni} signify the natural frequencies of the *n*-th mode in Hz and ε_1 and ε_i symbolize the axial strains. For a stay cable with an inclination angle θ, suppose that ΔT_P, ΔT_G, and ΔT_C denote the temperature variations of pylon, girder, and cable between the time instants t_1 and t_i. If the thermal gradient and the secondary effect due to structural constraints are negligible, the total variation of strain for this cable caused by these three temperature variations has been derived (Chen *et al*. 2014, Chen *et al*. 2015) as

$$\Delta \varepsilon = \varepsilon_i - \varepsilon_1 = \alpha_G \Delta T_G \cos^2 \theta + \alpha_P \Delta T_P \sin^2 \theta - \alpha_C \Delta T_C \tag{2}$$

where α_P, α_G, and α_C represent the thermal expansion coefficients of pylon, girder, and cable, respectively. For practical cases where the pylon and girder are commonly made of concrete and the steel cables are typically adopted, these thermal expansion coefficients can be approximated with the same value α. Combination of Eqs. (1) and (2) then yields

$$\frac{\Delta F}{F_1} = \frac{f_{ni}^2 - f_{n1}^2}{f_{n1}^2} \approx -\frac{\alpha}{\varepsilon_1}\left(\Delta T_C - \Delta T_G \cos^2 \theta - \Delta T_P \sin^2 \theta\right) = -\frac{\alpha}{\varepsilon_1} \Delta T_{eff} \tag{3}$$

According to Eq. (3), it is apparent that the variation in the square of cable frequency (and consequently the cable force variation) normalized to its reference value should be proportional to the effective temperature variation ΔT_{eff} incorporating the temperature effects from the pylon, girder, and cable. In Eq. (3), any single cable frequency is qualified for representing $\Delta F / F_1$. A statistical analysis (Chen *et al*. 2012) was conducted to determine the most significant mode usually observed for each cable and led to the uniform choice of the first modal frequency for each cable in the succeeding investigations.

Taking the one-month data of Cable E17 measured in Spring for example, $\Delta F / F_1$ is plotted in Fig. 2(b) together with the effective temperature variation ΔT_{eff} displayed in Fig. 2(a). Fig. 2 clearly indicates that $\Delta F / F_1$ generally follows a similar trend with ΔT_{eff} to verify the effectiveness of the above simplified analysis. Closer examination on Fig. 2 further reveals that there exists certain time shift between the variation of cable force and that of effective temperature. Additionally, the long-term baselines for both quantities demonstrated in Figs. 2(a) and 2(b) are not as consistent as their short-term (daily) counterparts.

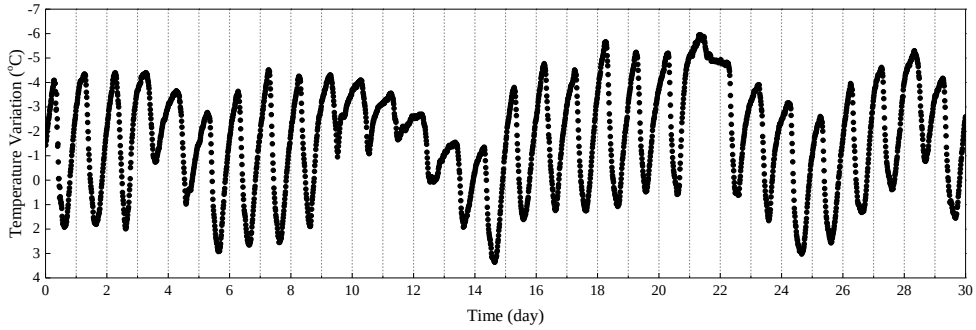

(a) Effective temperature variation

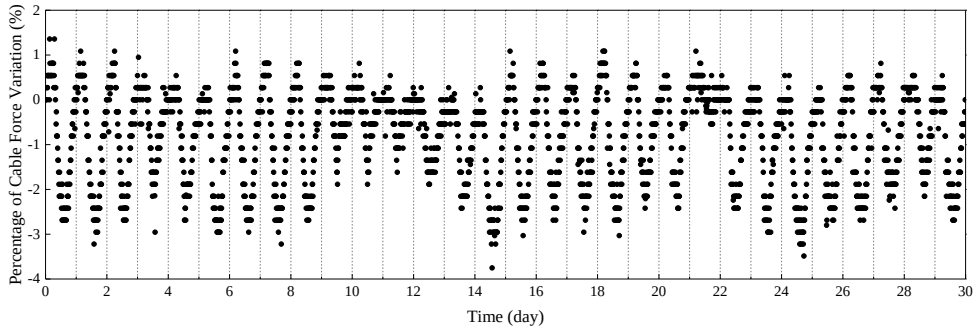

(b) Cable force variation

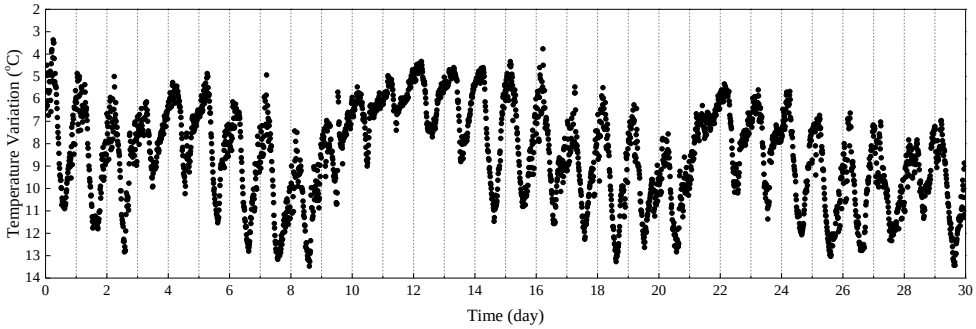

(c) Air temperature variation

Fig. 2 One-month data of Cable E17 measured in Spring

2.3 Decomposition of effective temperature and cable force

To systematically distinguish the daily and long-term temperature effects, EEMD was adopted to process the variation histories of cable force and effective temperature. Empirical mode decomposition (EMD) is an adaptive method to decompose a signal into several intrinsic mode functions (IMF) in balanced oscillations with respect to their zero means. The procedures of EMD usually start with constructing the upper and lower envelopes of the original signal by performing cubic spline interpolations to fit the local maxima and minima, respectively. The first round of sifting process is then completed by subtracting a temporary baseline taken as the average of both envelopes from the original signal. Repeatedly conducting such a sifting process would eventually yield an IMF and subtraction of the extracted IMF from the original signal will lead to the stage ready for decomposing the next IMF by similar sifting procedures. This process is reiterated until a monotonic signal, usually referred as the residue, is remained. Overall, the empirical mode decomposition of a signal can be mathematically expressed as

$$h(t) = \sum_{k=1}^{m} c_k(t) + r(t) \tag{4}$$

where $h(t)$ is the original signal, $c_k(t)$ denotes the k-th IMF, $r(t)$ symbolizes the residue, and m signifies the total number of obtained IMF's. It should be noted that the IMF's yielded from the EMD process earlier usually have the content in a higher frequency range. Adapted from EMD, EEMD is a noise-assisted data analysis method to ensure a narrowly-banded frequency content for each IMF (Wu and Huang 2009).

For the variations of effective temperature and cable force collected from Ai-Lan Bridge in each season, the previous analysis (Chen *et al*. 2014, Chen *et al*. 2015) demonstrated that 11 narrowly-banded IMF's together with the residue are consistently produced from the EEMD process. The first four IMF's for both quantities are all high-frequency measurement noises with trivial amplitudes and then filtered out in the subsequent analysis. Besides, it is clear that IMF 5 to IMF 8 of the effective temperature and the cable force are all primarily contributed by the frequency components at 1 cycle/day and 2 cycle/day. Accordingly, the combination of IMF 5 up to IMF 8 for each quantity is believed to represent the daily variation. On the other hand, the remained IMF 9 up to the residue undoubtedly indicate the long-term variation.

2.4 Correlation analysis

After classifying the effective temperature and cable force into two major components including the daily and the long-term variations, the correlation analysis was performed between the corresponding components of both quantities with the consideration of optimal time shift. For the selected data of Cables E10, E13, and E17 in all the four seasons, Table 1 summarizes the obtained values of correlation coefficient in different cases together with the associated optimal time shifts listed in the parenthesis. All the values of correlation coefficient of daily variation are no less than 0.97 in magnitude and their corresponding optimal time shifts range from 0 to 1.75 hr. Such a high value of correlation coefficient evidently discloses the almost perfect correlation between the daily variations of both quantities. It needs to be mentioned that the positive value of time shift signifies the moving of cable force toward the later time instant, while its negative value denotes the opposite. On the other hand, the values of correlation coefficient associated with

various cases of long-term variation are between -0.74 and -0.93 with a wider time shift range from -6.75 to 6.25 hr. Detailed results for varying the time shifts also indicate that the correlation coefficient is quite sensitive to the time shift in the case of daily variation, but relatively indifferent with the alternation of time shift in the case of long-term variation (Chen *et al*. 2015).

3. Exclusion of temperature effect from variation of cable force

The method reviewed in the previous section can serve as a convenient tool to effectively filter out the temperature effect on the variation of cable force. It is clear that the daily and long-term components of temperature variation demonstrate either highly or moderately linear correlation with the corresponding components of cable force variation. Therefore, the technique of least square errors are applied in the current section to determine the two different transfer coefficients associated with these two components of temperature variation for separating their possibly varied influences on the cable force variation. With the obtained transfer coefficients, the residual cable force variation after eliminating the environmental temperature effects are then presented.

3.1 Transfer coefficients for daily and long-term temperature variations

As indicated in Table 1, the optimal time shifts for the daily and long-term variations can be very different. This would lead to a dilemma in eliminating these two components of temperature variation from the cable force variation. Considering that the component of daily variation is much more sensitive to the time shift than that of long-term variation and it is usually with a dominant contribution, the optimal time shift $s\Delta t$ for the daily variation is taken for both components in the following analysis to decide the transfer coefficients.

At the time instant t_i, assume that $z_i = z(t_i)$ represents the denoised cable force variation. In addition, $x_{i-s} = x(t_i - s\Delta t)$ and $y_{i-s} = y(t_i - s\Delta t)$ denote the daily variation and the long-term variation of effective temperature with the same shift $s\Delta t$ along the time axis, respectively. To optimally exclude the effects of x_{i-s} and y_{i-s} from z_i in a linear manner, a transfer coefficient a_1 associated with the daily variation of effective temperature and another transfer coefficient a_2 associated with the long-term variation of effective temperature are to be determined such that the error between z_i and $a_1 x_{i-s} + a_2 y_{i-s}$ is minimized.

With the data collected at *n* consecutive time instants, an appropriate objective function for conducting the optimization procedures can be defined by the sum of the squares of the errors as

$$E = \sum_{i=s+1}^{n} \left(z_i - a_1 x_{i-s} - a_2 y_{i-s} - b\right)^2 \tag{5}$$

It should be particularly noted that the constant coefficient *b* in Eq. (5) is added to account for the possible inaccuracy at the initial reference time instant t_1 and the effects of other minor factors in addition to the temperature. Since both the cable force variation and the effective temperature variation are evaluated with respect to the corresponding quantities at t_1, the inaccurate initial values due to measurement noises can be conveniently adjusted by a constant shift to be determined. Moreover, the other minor factors to cause cable force variation may also deteriorate

the effectiveness of the obtained coefficients a_1 and a_2. The additional constant term would help to diminish this problem. In fact, the optimal values of a_1, a_2, and the constant coefficient b in Eq. (5) can be analytically solved from a system of three linear equations and hold the relation

$$b = \bar{z} - a_1\bar{x} - a_2\bar{y} \tag{6}$$

where

$$\bar{z} = \frac{1}{n-s}\sum_{i=s+1}^{n} z_i, \quad \bar{y} = \frac{1}{n-s}\sum_{i=s+1}^{n} y_i, \text{ and } \quad \bar{x} = \frac{1}{n-s}\sum_{i=s+1}^{n} x_i \tag{7}$$

In other words, the formulation of Eq. (5) is totally equivalent to

$$E = \sum_{i=s+1}^{n}\left[\left(z_i - \bar{z}\right) - a_1\left(x_{i-s} - \bar{x}\right) - a_2\left(y_{i-s} - \bar{y}\right)\right]^2 \tag{8}$$

Eq. (8) means that the linear regression analysis is performed by taking all the quantities with respect to the mean value of each variable. With this shift of reference point from the initial value to a more stable mean value, the possible problems induced by the initial inaccuracy and the other minor factors can be alleviated. Table 2 lists the optimal values of both transfer coefficients for Cables E10, E13, and E17 in all the four seasons. With no surprise, the transfer coefficient a_1 for the daily variation of effective temperature is regularly larger than a_2 for the long-term variation of effective temperature to reflect their relative contributions in the variation of cable force.

Table 1 Correlation coefficients and optimal time shifts of 3 stay cables based on the effective temperature

Cable Number	Season	Correlation coefficient (optimal time shift)	
		Daily variation	Long-term variation
E10	Spring	–0.98 (0.0 hr)	–0.83 (–6.25 hr)
	Summer	–0.97 (0.25 hr)	–0.78 (4.0 hr)
	Autumn	–0.97 (0.25 hr)	–0.83 (–6.75 hr)
	Winter	–0.98 (0.5 hr)	–0.87 (1.75 hr)
E13	Spring	–0.98 (1.25 hr)	–0.90 (–1.75 hr)
	Summer	–0.97 (1.0 hr)	–0.88 (6.0 hr)
	Autumn	–0.98 (1.5 hr)	–0.85 (–3.0 hr)
	Winter	–0.98 (1.75 hr)	–0.90 (5.5 hr)
E17	Spring	–0.99 (0.75 hr)	–0.92 (–0.5 hr)
	Summer	–0.99 (0.75 hr)	–0.91 (5.75 hr)
	Autumn	–0.99 (1.0 hr)	–0.93 (–1.0 hr)
	Winter	–0.98 (1.5 hr)	–0.93 (6.25 hr)

Table 2 Temperature transfer coefficients for three stay cables

Cable Number	Transfer coefficient for daily variation a_1				Transfer coefficient for long-term variation a_2			
	Spring	Summer	Autumn	Winter	Spring	Summer	Autumn	Winter
E10	–0.32	–0.32	–0.39	–0.47	–0.19	–0.11	–0.12	–0.21
E13	–0.49	–0.42	–0.61	–0.61	–0.20	–0.16	–0.15	–0.22
E17	–0.52	–0.50	–0.63	–0.67	–0.24	–0.20	–0.19	–0.24

3.2 Residual cable force variation after eliminating temperature effects

With the transfer coefficients displayed in Table 2, the residual cable force variation after the elimination of temperature effects can be obtained by $z_i - a_1 x_{i-s} - a_2 y_{i-s} - b$ for all the three stay cables in different seasons. Taking again the one-month data of Cable E17 measured in Spring for example, the values of residual cable force variation at different time instants are plotted in Fig. 3(a) with red crosses and their corresponding values before the elimination of temperature effects are also shown in grey dots. Fig. 3(a) evidently demonstrates that the range of cable force variation is significantly reduced from 5% to 2% with the elimination of temperature effects in this case. To verify the necessity of decomposing the effective temperature variation into two components and applying the time shift, Figs. 3(b) and 3(c) display the corresponding results without the former operation and without both operations, respectively. By comparing Figs. 3(a) and 3(b), it can be observed that the effectiveness of eliminating the temperature effects is declined without separating the daily and long-term variations even if the time shift is considered. The situation would get worse when the effective temperature variation is directly taken to determine the residual cable force variation without any time shift, as illustrated in Fig. 3(c). For further contrast, another formulation with the constant term b in Eq. (5) omitted to solve for the transfer coefficients is also adopted to produce the results shown in Fig. 3(d). The long-period fluctuation associated with the residual cable force variation in this figure clearly certifies the importance of including the constant term b in Eq. (5). Fig. 4 presents the residual cable force variations after eliminating the temperature effects for Cable E10 in all the four seasons. Similar to Fig. 3(a), the range of cable force variation is uniformly reduced from 4% to 2% in different cases to provide a more solid basis for the subsequent damage detection.

4. Thresholds and criteria for damage detection

As indicated in Fig. 4, the maximum duration of the continuous data collected in this study for Spring, Summer, Autumn, and Winter are 30 days, 21 days, 22 days, and 30 days, respectively. The EEMD process to separate the daily component with the long-term component and the subsequent elimination of temperature effects to obtain the residual cable force variation were both carried out with such a maximum duration in the previous section simply for demonstrations. To determine the thresholds beyond which the probability of damage occurrence is high and then

establish the appropriate criteria for damage detection in this section, succeeding data with a sufficient length are required for further statistical analysis. Accordingly, the monitoring data with a shorter length of 7 days are adopted in the subsequent EEMD analysis. It should be emphasized that this selected length of 7 days is generally adequate because only the final 24 data points with a time duration of 6 hours from the EEMD analysis at each time instant are considered in the current study for damage detection.

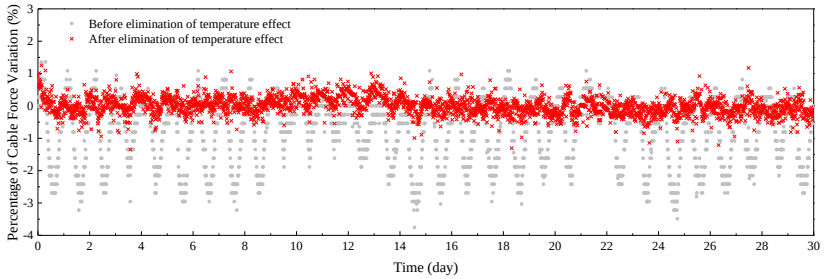

(a) Elimination with decomposition and shift

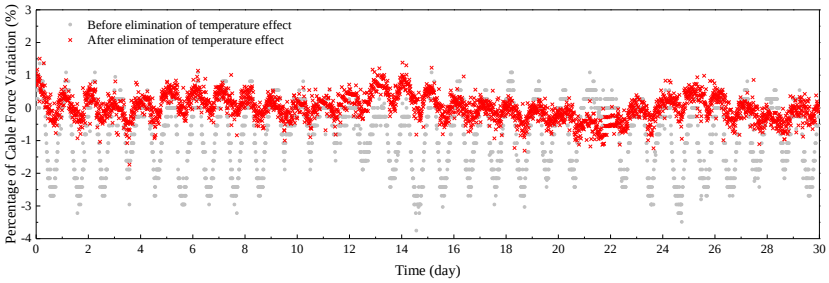

(b) Elimination without decomposition but with shift

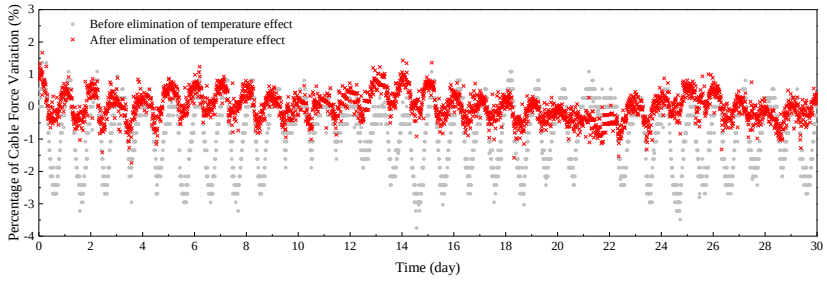

(c) Elimination without decomposition and shift

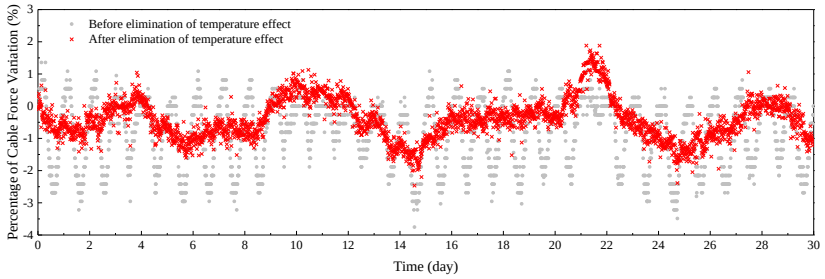

(d) Elimination without constant term

Fig. 3 Residual cable force variation of Cable E17 in Spring

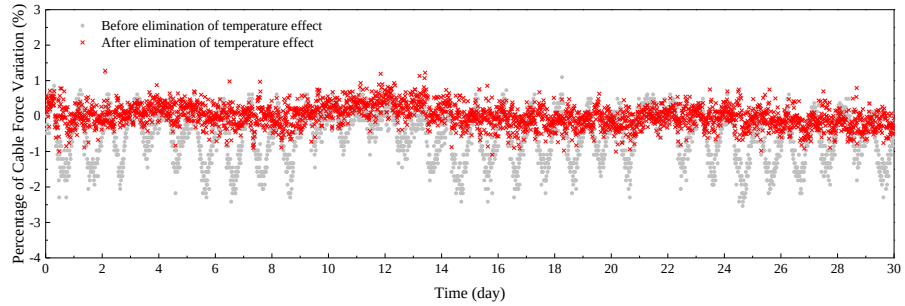

(a) Spring

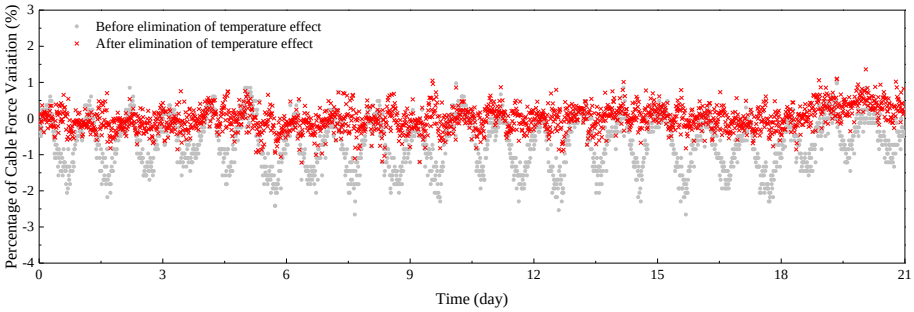

(b) Summer

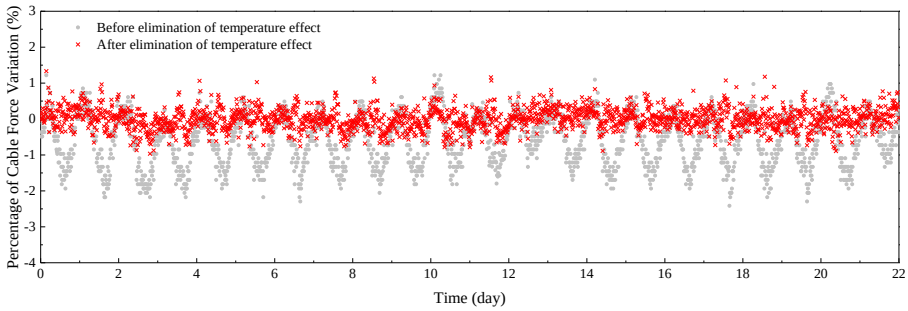

(c) Autumn

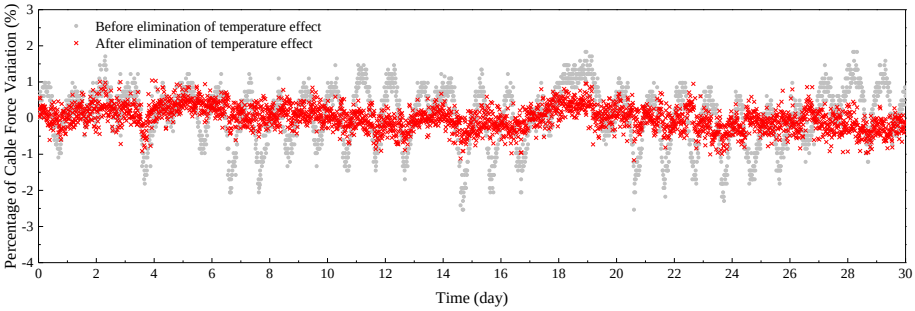

(d) Winter

Fig. 4 Residual cable force variation of Cable E10 in four seasons based on the effective temperature

4.1 Thresholds for different levels of exceedance probability

Also taking the one-month data of Cable E17 in Spring as an example and considering the time shift, a progress with one point at a time is made to move along the time axis for obtaining all the possible 2206 time histories with a length of 7 days. The process of eliminating the temperature effects as described in the previous section is then conducted for each pair of effective temperature variation and cable force variation. The residual cable force variations resulted from all the 2206 events cover a wide range of different cases to give a good database for determining the thresholds with certain exceedance probabilities. Since the damage criteria described in the next subsection will be based on the most recent 24 points (6 hours), a consistent selection of the last 24 points of each residual cable force variation is also adopted here to perform the statistical analysis for obtaining different levels of thresholds. In other words, there are totally 24×2206 points of data yielded by this example of Cable E17 measured in Spring.

For a set of data following the normal distribution with a zero mean and a standard deviation σ, the probabilities for values to exceed 2σ and 3σ are 5% and 0.3%, respectively. The former is usually considered as a relatively high threshold and the latter corresponds to an extremely high one. Even though the residual cable force variations as displayed in Fig. 4 are not perfectly in a normal distribution, the two levels with 5% and 0.3% of exceedance probability can still be taken as crucial reference thresholds to establish the damage criteria. Furthermore, Fig. 4 also illustrates that the residual cable force variation is not distributed in a well symmetric manner with respect to the zero axis. To construct relatively sensitive damage criteria, more specific thresholds for the upper (positive) part and the lower (negative) part of residual cable force variation are determined in this study. The upper and lower thresholds with 0.3% and 5% of exceedance probabilities are summarized in Table 3 for Cables E10, E13, and E17 in different seasons. As expected, the results in Table 3 exhibit that the 5% thresholds are more consistent in different seasons and with a narrower lower-to-upper range than those with 0.3% of exceedance probability. The comparison among different stay cables further reveals that the range between the lower and upper thresholds is the widest for Cable E13 and narrower for Cables E10 and E17 in either the case of 0.3% or 5% exceedance probability.

4.2 Upper and lower criteria for damage detection

For detecting the instantly occurred damages, the first decision to make is the examined duration of the most recent history. The choice of an overlong period will dilute the effect of damage in its new occurrence and delay the detection time. On the other hand, the inspected points of data will be too limited to make a statistical sense if an extremely short period is selected. In the current research, this duration is set at 6 hours (24 points) for a good balance. Other critical issues for damage detection include the choice of a higher or lower threshold and the selection of criteria in a continuous or cumulative manner. In general, a larger damage is easier to be detected with a continuous criterion based on a higher threshold, while a smaller damage intends to be more conveniently distinguished with a cumulative criterion based on a relatively lower threshold. To cover the detection for different levels of damage, four criteria with either 5% or 0.3% threshold and either checking cumulative or continuous exceeding points are established. Moreover, these four criteria will be respectively decided for the upper part and the lower part of residual cable force variation to improve their sensitivity.

Table 3 Thresholds with 0.3% and 5% of exceedance probabilities based on the effective temperature

Cable Number	Threshold for 5% exceedance probability				Threshold for 0.3% exceedance probability			
	Spring	Summer	Autumn	Winter	Spring	Summer	Autumn	Winter
E10	>0.65	>0.79	>0.64	>0.60	>1.16	>1.18	>1.07	>0.98
	<-0.68	<-0.72	<-0.67	<-0.79	<-0.99	<-1.16	<-0.92	<-1.26
E13	>1.02	>1.05	>0.89	>0.83	>1.61	>1.71	>1.43	>1.21
	<-0.85	<-0.82	<-0.92	<-0.94	<-1.34	<-1.25	<-1.55	<-1.39
E17	>0.62	>0.74	>0.60	>0.58	>1.01	>1.36	>1.03	>0.91
	<-0.71	<-0.72	<-0.71	<-0.90	<-1.24	<-1.05	<-1.15	<-1.38

Similar to the work for the determination of thresholds in the previous subsection, the residual cable force variations obtained from all the possible extractions of the recorded time histories are taken for statistical analysis. The last 24 points of each case are firstly checked for evaluating the total number and the longest continuous number to exceed the 5% or 0.3% threshold. The largest value in all the possible cases for each category is then searched to represent the worst scenario when the bridge still stays in the healthy condition. The maximum number in each category is finally added by one to serve as a criterion for indicating the occurrence of possible damages. Table 4 lists all the four upper criteria for the three cables in different seasons and the corresponding lower criteria are presented in Table 5. Also as expected, the required number for the 0.3% criterion is smaller than the corresponding 5% criterion and so is the continuous criterion compared to its corresponding cumulative criterion. The noticeable difference between the results in Tables 4 and 5 further validates the necessity of separating the upper and lower criteria.

Table 4 Number of exceeding points for each of the four upper criteria

Cable No.	Number of points to exceed the 5% upper threshold								Number of points to exceed the 0.3% upper threshold							
	Cumulative				Continuous				Cumulative				Continuous			
	Spr	Sum	Aut	Win	Spr	Sum	Aut	Win	Spr	Sum	Aut	Win	Spr	Sum	Aut	Win
E10	13	10	8	11	8	4	3	4	4	3	2	5	2	3	2	2
E13	6	7	7	8	4	3	3	3	3	4	3	3	2	3	2	2
E17	11	16	15	13	5	13	7	7	3	3	2	2	2	2	2	2

Table 5 Number of exceeding points for each of the four lower criteria

Cable No.	Number of points to exceed the 5% upper threshold								Number of points to exceed the 0.3% upper threshold							
	Cumulative				Continuous				Cumulative				Continuous			
	Spr	Sum	Aut	Win	Spr	Sum	Aut	Win	Spr	Sum	Aut	Win	Spr	Sum	Aut	Win
E10	8	8	8	14	4	6	8	7	2	3	3	4	2	2	2	2
E13	12	11	9	11	10	6	7	11	3	3	2	7	2	2	2	7
E17	13	15	9	13	11	10	6	10	2	4	2	5	2	2	2	5

5. Simulated damage detection by eliminating effective temperature

With the upper and lower criteria established in the previous section, the detection of sudden cable force changes caused by instant damages occurred in cable-stayed bridges can be conveniently conducted. The next problem to investigate is the sensitivity of this methodology, i.e., the minimum level of cable force change that can be detected. In addition, the effectiveness of different criteria and the required time to detect a certain level of damage are also important issues deserving detailed examinations. For extensively exploring these questions, the monitoring data for the three stay cables in different seasons are adopted to simulate various possible damage scenarios. In each simulation, a certain percentage of increased or decreased cable force is applied at a particular time instant and from then on. Starting from the instant that damage firstly occurs, the detection procedures are carried out for each simulation by progressing one point at a time along the time axis to check all the criteria. This action is continued until at least one criterion is reached or 48 time increments (12 hours) have passed. The reason to stop at 12 hours is that it is hoped to identify the damage before such an elapsed time and any time longer than that will be considered as unsuccessful damage detection. Taking the one-month data shown in Fig. 3(a) for Cable E17 measured in Spring as an example, the 2206 time instants after the first 7 days provide a total of 2158 simulations by saving the last 48 points for the movement of damage detection. All these different simulations will basically cover most of the diverse situations for the occurrence of damages.

In this section, three levels of sudden cable force change including ±1%, ±1.5%, and ±2% are examined. It is firstly found that the ±1% cable force changes cannot be identified in 12 hours for most of the possible simulations. On the other hand, all the simulations for the cases of ±1.5% and ±2% are successfully detected with at least one damage criterion activated in less than 12 hours. To investigate the effectiveness of different criteria, the percentage for each of the four upper/lower criteria to be firstly activated under positive/negative cable force changes is inspected. The results for the three cables in different seasons under +1.5% and +2% damages are listed in Tables 6 and 7, respectively. It should be noted that the summed percentage of all the four criteria in each case is typically larger than 100% because more than one criterion may be simultaneously activated. From Tables 6 and 7, it can be observed that each criterion has the chance to be firstly reached in different cases. This confirms the necessity to check four different criteria for more effective damage detection. Furthermore, the continuous criterion with the 0.3% threshold is

dominant for most of the cases under a larger damage (+2%), while more widespread triggering exists in the cases under a smaller damage (+1.5%). The results corresponding to the negative cable force changes also show similar trends.

In evaluating the required time to detect a certain level of damage, the time lags (positive time shifts) for the daily component of effective temperature ranging from 0 to 1.75 hr as listed in Table 1 need to be included. Moreover, it can be expected that the detection of a smaller damage level (±1.5%) may require as long as 6 hours such that all the 24 examined points are fully affected by the damage to pass the adopted criteria. As for the cases subjected to a larger damage (±2%), the same criteria are possibly reached when only part of the totally 24 examined points are influenced by the damage. Table 8 summarizes the longest time to detect the damage among all the simulations for each case together with the corresponding average time listed in the parenthesis. It is obvious that the required damage detection time under a smaller damage (±1.5%) is usually longer than that under a larger damage (±2%) no matter in the worst scenario or in the average sense. With the combination of the two factors mentioned above to determine the damage detection time, it is certainly reasonable that the cases with ±2% of cable force change can be identified within 6 hours and those with ±1.5% of cable force change can be detected within 9 hours. Majorly due to the time lag length of effective temperature for different cables, it is also evident that the damage detection time increases with the order of Cable E10, Cable E17, and Cable E13.

Table 6 Percentages for the upper criteria to be firstly activated under +1.5% damage

Cable No.	Percentage to be firstly activated with the 5% upper threshold								Percentage to be firstly activated with the 0.3% upper threshold							
	Cumulative				Continuous				Cumulative				Continuous			
	Spr	Sum	Aut	Win	Spr	Sum	Aut	Win	Spr	Sum	Aut	Win	Spr	Sum	Aut	Win
E10	0	1	0	0	4	34	23	12	5	84	90	0	97	68	82	94
E13	25	11	4	2	58	93	60	43	9	1	5	10	37	11	48	70
E17	1	5	0	0	6	8	4	1	11	24	98	99	96	85	85	88

Table 7 Percentages for the upper criteria to be firstly activated under +2% damage

Cable No.	Percentage to be firstly activated with the 5% upper threshold								Percentage to be firstly activated with the 0.3% upper threshold							
	Cumulative				Continuous				Cumulative				Continuous			
	Spr	Sum	Aut	Win	Spr	Sum	Aut	Win	Spr	Sum	Aut	Win	Spr	Sum	Aut	Win
E10	0	1	0	0	0	7	3	1	1	98	99	0	100	94	96	100
E13	4	2	1	1	20	98	24	13	11	2	4	5	86	52	83	93
E17	0	0	0	0	0	0	0	0	4	8	100	100	100	99	96	95

Table 8 Average (longest) time to detect different levels of damage based on the effective temperature

Cable No.	Average (longest) time to detect the damage (hr)															
	+1.5% cable force				–1.5% cable force				+2% cable force				–2% cable force			
	Spr	Sum	Aut	Win	Spr	Sum	Aut	Win	Spr	Sum	Aut	Win	Spr	Sum	Aut	Win
E10	0.7	1.1	0.8	1.1	0.5	1.1	0.8	1.3	0.5	1.0	0.7	1.0	0.5	0.8	0.7	1.0
	(3.5)	(3.5)	(2.5)	(4.3)	(3.0)	(4.0)	(1.8)	(5.3)	(1.5)	(2.0)	(1.0)	(1.8)	(1.0)	(1.8)	(1.3)	(1.8)
E13	2.5	2.2	2.4	2.6	2.2	2.0	2.8	4.4	1.9	1.8	2.1	2.3	1.8	1.5	2.1	3.6
	(6.0)	(8.5)	(6.8)	(7.0)	(7.8)	(8.8)	(6.5)	(7.8)	(4.0)	(3.5)	(4.5)	(5.5)	(3.3)	(3.3)	(3.8)	(5.0)
E17	1.4	2.0	1.6	2.2	1.5	1.5	1.6	3.5	1.3	1.3	1.5	2.0	1.2	1.3	1.5	2.8
	(4.5)	(8.3)	(4.0)	(6.8)	(5.3)	(6.8)	(3.0)	(7.0)	(2.0)	(3.8)	(1.8)	(3.8)	(2.0)	(1.8)	(1.8)	(4.0)

6. Simulated damage detection by eliminating air temperature

The damage detection methodology developed in the current study is further explored in this section to consider the frequently encountered situations where simply the air temperature is measured by the SHM system. Instead of adopting the effective temperature defined in Eq. (3) for a more comprehensive elimination of environmental effects, the temperature measurement of surrounding air provided by the original monitoring system of Ai-Lan Bridge is employed to perform the detection of sudden cable force changes. Taking again the monitoring data of Cable E17 in Spring for example, the corresponding air temperature variation ΔT_a is plotted in Fig. 2(c) to compare with the effective temperature variation depicted in Fig. 2(a) and the cable force variation displayed in Fig. 2(b). It can be observed that the trend of ΔT_a goes in advance of ΔT_{eff} and even ahead of $\Delta F / F_1$. This phenomenon is physically reasonable because the variations of cable force and structural temperature should be induced by the variation of the ambient air temperature.

First, the EEMD process is conducted to decompose the air temperature variation into 11 narrowly-banded IMF's together with the residue. The same correlation analysis as described in Subsection 2.4 is then performed between the corresponding daily and the long-term components of the air temperature variation and the cable force variation with the consideration of optimal time shift. Table 9 summarizes the obtained values of correlation coefficient for the three selected stay cables in all the four seasons together with the associated optimal time shifts. In comparison with the results in Table 1, it is apparent that both the correlation coefficients of daily variation and long-term variation in Table 9 are not as high as those based on the effective temperature variation. All the values of the correlation coefficient for daily variation in this case, however, still fall in the range between –0.91 and –0.99 to indicate excellent correlation. In addition, the optimal time shifts for the daily components in Table 9 are all less than their corresponding values in Table 1 and most of them are with negative values. This fact again shows that the cable force variation typically falls behind that of air temperature. The procedures in Subsection 3.1 are subsequently

followed to determine the transfer coefficients a_1 for the daily variation of air temperature and a_2 for the long-term variation. With the obtained transfer coefficients in each case, the residual cable force variation after the elimination of temperature effects can be constructed for all the three stay cables in different seasons. Fig. 5 illustrates the results after eliminating the temperature effects based on the air temperature for Cable E10. In this case, the range of cable force variation is uniformly reduced from 4% to around 2.5% in different seasons, a little more widespread than the corresponding results shown in Figure 4 based on the effective temperature.

The succeeding step next goes to apply the process explicated in Subsection 4.1 to determine the upper and lower thresholds with 0.3% and 5% of exceedance probabilities summarized in Table 10. Comparison of Table 10 and Table 3 unsurprisingly reveals that the range between the lower and upper thresholds is mostly wider if the analysis is based on the air temperature. Similar to the effort in Subsection 4.2, four criteria with either 5% or 0.3% threshold and either cumulative or continuous manner can then be constructed respectively for the upper part and the lower part of residual cable force variation. Finally, the detection of sudden cable force changes are performed with these established upper and lower criteria. In this section, three levels of sudden cable force change including ±1.5%, ±2%, and ±2.5% are examined. It is discovered that the ±1.5% cable force changes cannot be identified in 12 hours for several of the possible simulations. The longest time to detect the damage together with the corresponding average time for the three cables in different seasons under +2% and +2.5% damages are listed in Table 11. Like the results presented in Table 8 based on the effective temperature, the required damage detection time under a smaller damage (±2%) is normally longer than that under a larger damage (±2.5%) no matter in the worst scenario or in the average sense. Overall, the cases with ±2.5% of cable force change can be identified in 4 hours and those with ±2% of cable force change can be detected in 12 hours.

Table 9 Correlation coefficients and optimal time shifts of 3 stay cables based on the air temperature

Cable Number	Season	Correlation coefficient (optimal time shift)	
		Daily variation	Long-term variation
E10	Spring	–0.94 (–0.75 hr)	–0.77 (19.75 hr)
	Summer	–0.91 (–0.5 hr)	–0.52 (12.0 hr)
	Autumn	–0.96 (–1.5 hr)	–0.81 (8.5 hr)
	Winter	–0.96 (–1.5 hr)	–0.89 (6.5 hr)
E13	Spring	–0.94 (0.5 hr)	–0.70 (24.0 hr)
	Summer	–0.93 (0.25 hr)	–0.42 (15.25 hr)
	Autumn	–0.98 (–0.25 hr)	–0.84 (18.25 hr)
	Winter	–0.96 (–0.25 hr)	–0.82 (10.5 hr)
E17	Spring	–0.96 (0.0 hr)	–0.64 (27.25 hr)
	Summer	–0.96 (0.25 hr)	–0.34 (15.25 hr)
	Autumn	–0.99 (–0.75 hr)	–0.83 (19.5 hr)
	Winter	–0.96 (–0.5 hr)	–0.80 (11.5 hr)

Comparison of Table 8 and Table 11 further unveils that the damage detection time based on the air temperature is unexpectedly shorter than that based on the effective temperature for certain cases with ±2% change of cable force. Such a phenomenon seems to contradict with the more widespread distribution range after elimination based on the air temperature, as demonstrated in Fig. 5. Nevertheless, the commonly negative value for the optimal time shift listed in Table 9 to gain the advantage in avoiding the time lag for the damage detection based on the air temperature would provide a logical explanation.

Table 10 Thresholds with 0.3% and 5% of exceedance probabilities based on the air temperature

Cable Number	Threshold for 5% exceedance probability				Threshold for 0.3% exceedance probability			
	Spring	Summer	Autumn	Winter	Spring	Summer	Autumn	Winter
E10	>0.80	>0.81	>0.66	>0.74	>1.08	>1.27	>1.08	>1.10
	<-0.84	<-0.93	<-0.60	<-0.81	<-1.25	<-1.34	<-0.85	<-1.33
E13	>1.35	>1.08	>0.92	>1.03	>1.97	>1.66	>1.50	>1.48
	<-1.04	<-1.17	<-0.85	<-1.07	<-1.57	<-1.60	<-1.36	<-1.61
E17	>1.03	>0.92	>0.73	>0.91	>1.37	>1.32	>1.11	>1.29
	<-1.09	<-1.19	<-0.72	<-1.09	<-1.62	<-1.64	<-1.06	<-1.66

Table 11 Average (longest) time to detect different levels of damage based on the air temperature

Cable No.	Average (longest) time to detect the damage (hr)															
	+2% cable force				2% cable force				+2.5% cable force				2.5% cable force			
	Spr	Sum	Aut	Win	Spr	Sum	Aut	Win	Spr	Sum	Aut	Win	Spr	Sum	Aut	Win
E10	0.5	0.8	0.5	0.5	0.5	0.8	0.5	0.8	0.5	0.7	0.5	0.5	0.5	0.7	0.5	0.7
	(1.8)	(2.5)	(1.0)	(2.5)	(2.0)	(2.3)	(0.8)	(2.3)	(0.8)	(1.5)	(0.5)	(1.0)	(1.0)	(1.3)	(0.5)	(1.5)
E13	1.9	1.2	0.6	1.0	2.1	1.3	0.8	1.7	1.4	1.0	0.5	0.8	1.6	1.0	0.8	1.1
	(9.8)	(5.5)	(2.3)	(5.0)	(11.8)	(3.8)	(2.3)	(5.8)	(4.0)	(2.5)	(1.3)	(3.0)	(4.5)	(1.8)	(1.3)	(2.5)
E17	1.5	1.7	0.5	0.7	1.3	2.0	0.5	1.8	1.0	1.3	0.5	0.5	0.5	1.3	0.5	1.1
	(10.3)	(7.3)	(1.8)	(5.8)	(11.3)	(11.3)	(1.0)	(9.5)	(3.0)	(3.5)	(0.5)	(3.5)	(2.8)	(3.0)	(0.5)	(2.8)

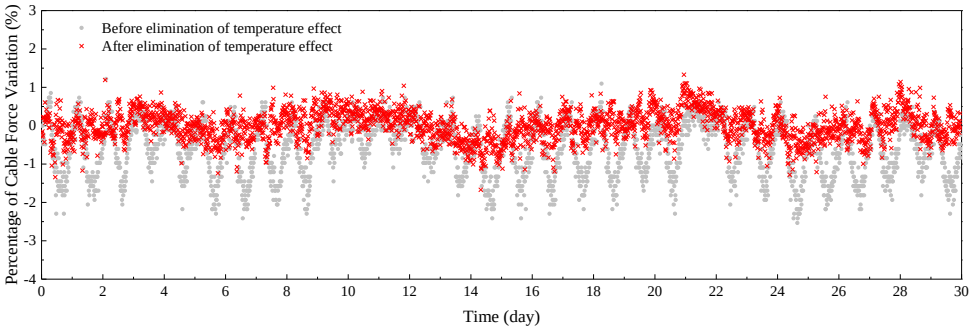

(a) Spring

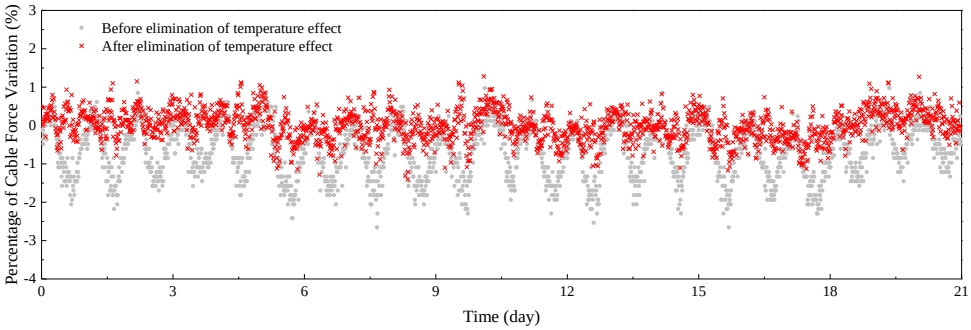

(b) Summer

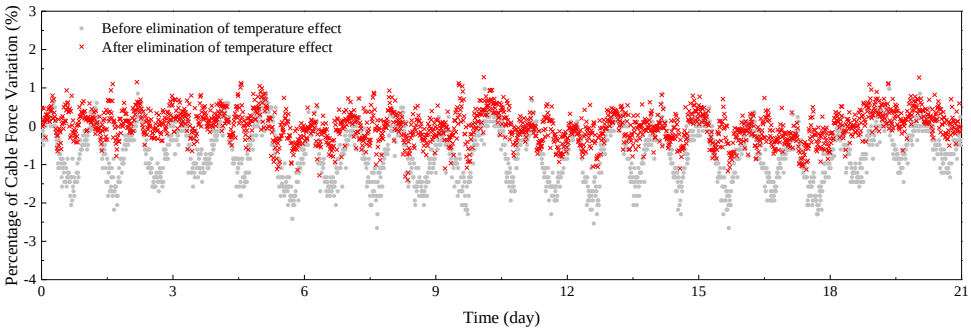

(c) Autumn

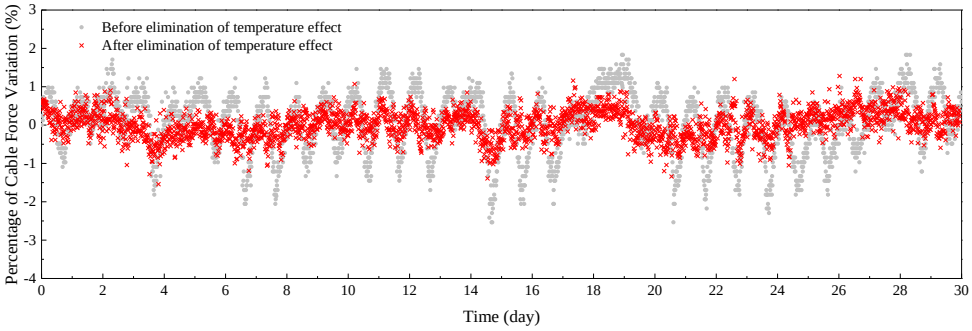

(d) Winter

Fig. 5 Residual cable force variation of Cable E10 in four seasons based on the air temperature

7. Conclusions

This study firstly determines two transfer coefficients for the daily and long-term components of effective temperature variation to eliminate the environmental temperature effects from the cable force variation. In the optimization process of solving the transfer coefficients, it is clearly demonstrated that each variable needs to be evaluated with respect to its mean value for cleanly excluding the temperature effects. In general, the residual cable force variations of different cases can be consistently reduced to a narrow range of 2%. It is also exhibited that specific thresholds for the upper part and the lower part of residual cable force variation are required to construct more sensitive damage criteria. The application of four criteria according to 5% or 0.3% exceeding threshold and cumulative or continuous basis is further validated to successfully cover the detection for different levels of damage. The simulated results to consider various damage scenarios unambiguously indicate that the damages with cable force changes larger than ±1% can be confidently detected with the proposed methodology. This 1% detection limit has no doubts coming from the half range of the residual cable force variation. More specifically, the continuous criterion with the 0.3% threshold is firstly reached for most of the cases under a larger damage. On the other hand, the first triggering criterion is more diversified in the cases under a smaller damage. As for the required time to detect damage, it is found that the cases with ±2% of cable force change can be discovered in no more than 6 hours and those with ±1.5% of cable force change can be identified in at most 9 hours. Such a length of detection time in the worst scenario essentially makes good sense in engineering practice for an insignificant level of sudden cable force change either at ±2% or ±1.5%.

This methodology is also investigated for more lightly monitored cases where only the air temperature measurement is available. Under such circumstances, the residual cable force variations typically fall into a slightly wider range of 2.5%. The corresponding simulated results further show that the damages with cable force changes larger than ±1.5% can be detected based on the air temperature. This deteriorated detection limit is obviously caused by the more dispersive characteristic of the residual cable force variation. Therefore, the more convenient approach simply based on the air temperature measurement also offers a feasible solution for the damage detection of cable-stayed bridges, but with a trade-off in sensitivity. Even though not exhaustively reflecting the environmental temperature effects on the cable force variation, both the effective temperature and the air temperature can be considered as valid indices to eliminate these effects at high and low monitoring costs.

The developed method in this research provides a keystone for detecting the instant damages in the health monitoring of cable-stayed bridges. Additional effort to quantify the corresponding cable force changes caused by various damage patterns is underway for assessing the applicability of this method in practical bridges with its 1% detection limit. A generalization of the current work is also in progress to include the detection of the long-term damages gradually accumulated. Moreover, it will be further explored to investigate the possibility of reducing the damage detection time with a sampling interval less than 15 minutes. Ultimately, the collection of a much longer period of continuous measurements is expected to be feasible in the future for a more accurate elimination of temperature effects to detect smaller damages.

Acknowledgments

The authors are grateful to the financial support from the Ministry of Science and Technology of Republic of China under Grant NSC100-2221-E-224-049, Grant NSC 101-2221-E-224-061 and Grant NSC102-2221-E-224-043.

References

Cao, Y.H., Yim, J.S., Zhao, Y. and Wang, M.L. (2011), "Temperature effects on cable stayed bridge using health monitoring system: a case study", *Struct. Health. Monit.*, **10**(5), 523-537.

Chen, C.C., Wu, W.H. and Liu, C.Y. (2012), "Effects of temperature variation on cable forces of an extradosed bridge", *Proceedings of 6th European Workshop on Structural Health Monitoring*, Dresden, Germany, July**.**

Chen, C.C., Wu, W.H. and Liu, C.Y. (2014), "Decomposed components of the effective temperature history and their correlation with the variation of stay cable force", *Proceedings of the 7th European Workshop on Structural Health Monitoring*, Nantes, France, July.

Chen, C.C., Wu, W.H. and Liu, C.Y. (2015), "Daily and long-term variations of the effective temperature history and their correlation with those of stay cable force", *Proceedings of the 2nd International Conference on Sustainable Urbanization*, Hong Kong, January.

Chen C.C., Wu, W.H. and Shih, Y.D. (2010), "Effects of environmental variability on stay cable frequencies", *Proceedings of the 2nd International Symposium on Life-Cycle Civil Engineering*, Taipei, Taiwan, October.

Chen, C.C., Wu, W.H. and Tseng, H.Z. (2008), "Measurement of ambient vibration signal of shorter stay cables from stressing to service stages", *Proceedings of the 4th European Workshop on Structural Health Monitoring*, Krakow, Poland, July.

Cunha, A., Caetano, E., Magalhaces, F. and Moutinho, C. (2013), "Recent perspectives in dynamic testing and monitoring of bridges", *Struct. Control Health*., **20**(6), 853-877.

Degrauwe, D., De Roeck, G. and Lombaert, G. (2009), "Uncertainty quantification in the damage assessment of a cable-stayed bridge by means of fuzzy numbers", *Comput. Struct.*, **87**(17-18), 1077-84.

Ding, Y.L., Li, A.Q. and Deng, Y. (2010), "Structural damage warning of a long-span cable-stayed bridge using novelty detection technique based on wavelet packet analysis", *Adv. Struct. Eng.*, **13**(2), 291-298.

Ding, Y.L., Wang, G.X., Zhou, G.D. and Li, A. (2013), "Life-cycle simulation method of temperature field of steel box girder for Runyang cable-stayed bridge based on field monitoring data", *China Civil Eng. J.*, **46**(5), 129–136.

Dohler, M., Hille, F., Mevel, L. and Rucker, W. (2014), "Structural health monitoring with statistical method during progressive damage test of S101 bridge", *Eng. Struct*., **69**, 183-193.

Li, H.J. (2009), "Temperature effect analysis for structural state estimation of PC cable-stayed bridge", *Archit. Env. Eng.*, **31**(5), 81-85.

Min, Z.H., Sun, L.M. and Dan, D.H. (2009), "Effect analysis of environmental factors on structural modal parameters of a cable-stayed bridge", *J. Vib. Shock*, **28**(10), 99-105.

Min, Z.H., Sun, L.M. and Zhong, Z. (2011), "Effect analysis of environmental temperature on dynamic properties of cable- stayed bridge", *J. Tongji. U.*, **39**(4), 488-494.

Ni, Y.Q., Hua, X.G., Fan, K.Q. and Ko, J.M. (2005), "Correlating modal properties with temperature using long-term monitoring data and support vector machine technique", *Eng. Struct.*, **27**(12), 1762-73.

Ni, Y.Q., Hua, X.G., Wong, K.Y. and Ko, J.M. (2007), "Assessment of bridge expansion joints using long-term displacement and temperature measurement", *J. Perform Constr. Facil. - ASCE*, **21**(2), 143-151.

Ni, Y.Q., Zhou, H.F., Chan, K.C. and Ko, J.M. (2008), "Modal flexibility analysis of cable-stayed Ting Kau bridge for damage identification", *Comput.-Aided Civ. Infrastruct. Eng*., **23**(3), 223-236.

Ni, Y.Q., Zhou, H.F. and Ko, J.M. (2009), "Generalization capability of neural network models for temperature-frequency correlation using monitoring data", *J. Struct. Eng. - ASCE*, **135**(10), 1290-1300.

Sun, L.M., Zhou, Y. and Li, X.L. (2012), "Correlation study on modal frequency and temperature effects of a cable-stayed bridge model", *Adv. Mater. Res.*, **446-449**, 3264-3272.

Trker, T. and Bayraktar, A. (2014), "Structural safety assessment of bowstring type RC arch bridges using ambient vibration testing and finite element model calibration", *Measurement*, **58**, 33-45.

Whelan, M.J. and Janoyan, K.D. (2010) "In-service diagnostics of a highway bridge from a progressive damage case study", *J. Bridge Eng. - ASCE*, **15**(5), 597-607.

Wu, Z.H. and Huang, N.E. (2009), "Ensemble empirical mode decomposition: a noise-assisted data analysis method", *Adv. Adapt. Data Anal.*, **1**(1), 1-41.

Xu, Z.D. and Wu, Z.S. (2007), "Simulation of the effect of temperature variation on damage detection in a long-span cable-stayed bridge", *Struct. Health Monit.*, **6**(3), 177-189.

Yao, C. and Li, Y.D. (2012), "Research on temperature influences in cable-stayed bridges' health monitoring", *Appl. Mech. Mater.*, **188**, 162-167.

Zhou, H.F., Ni, Y.Q. and Ko, J.M. (2010), "Constructing input to neural networks for modeling temperature-caused modal variability: mean temperatures, effective temperatures, and principal components of temperatures", *Eng. Struct.*, **32**(6), 1747-1759.

Zhou, H.F., Ni, Y.Q. and Ko, J.M. (2012), "Eliminating temperature effect in vibration-based structural damage detection", *J. Eng. Mech. - ASCE*, **137**(12), 785-796.

Zhou, Y., Sun, L.M. and Sun, S.W. (2013), "Temperature field and its effects on a long-span steel cable-stayed bridge based on monitoring data", *Proceedings of the 13th East Asia-Pacific Conference on Structural Engineering and Construction*, Sapporo, Japan, September.